Supporting Information for "Attribution of observed recent decrease in low clouds over the northeastern Pacific to cloud-controlling factors"

Hendrik Andersen[1,2], Jan Cermak[1,2], Lukas Zipfel[1,2], Timothy A. Myers[3,4]

[1]Karlsruhe Institute of Technology (KIT), Institute of Meteorology and Climate Research, Karlsruhe, Germany

[2]Karlsruhe Institute of Technology (KIT), Institute of Photogrammetry and Remote Sensing, Karlsruhe, Germany

[3]Cooperative Institute for Research in Environmental Sciences (CIRES), University of Colorado, Boulder, USA

[4]Physical Science Laboratory, National Oceanic and Atmospheric Administration, Boulder, USA

Contents of this file

1. Figures S1 to S6
2. Tables S1 and S2

Introduction

This file contains supporting information documenting:

Figure S1: Near-global map of LCC trend patterns from MODIS data between 2001 and 2020.

Figure S2: Trend patterns of LCC between 2003 and 2020 in the Aqua MODIS data, and a comparison to Terra MODIS data.

Figure S3: Average LCC of Terra and Aqua MODIS, and their differences for the time period with mutual data (2003–2020).

Figure S4: Map showing trend patterns of relative humidity at 1000 hPa in the northeastern Pacific from ERA5 data between 2001 and 2020.

Figure S5: Maps showing trend patterns of specific humidity at 1000 hPa and 700 hPa in the northeastern Pacific from ERA5 data between 2001 and 2020.

Figure S6: Boxplots showing the RMSE in independent test data between different sampling techniques for the 6 and 7-CCF setups and all models.

Table S1: Details on the hyperparameter tuning of the XGB models.

Table S2: Details on the hyperparameter tuning of the ANN models.

Table S1. Hyperparameter tuning of the XGB model. The left-hand column names the property, and the right-hand column lists the values tested using random grid search for 100 iterations. Bold values are chosen for the final model on the basis of a 10-fold cross validation.

Hyperparameter	**XGB with 6 CCFs**	**XGB with 6 CCFs**
Learning rate	[0.001,0.003,0.01,0.03,0.1,**0.3**]	[0.001,0.003,0.01,**0.03**,0.1,0.3]
Max. depth	[2, 3, 4, 5, **6**, 7]	[2, 3, 4, 5, 6, **7**]
Num. of estimators	[**100**, 200, 300, 400, 500]	[100, **200**, 300, 400, 500]
Reg. param. λ	[0.01, 0.03, 0.1, 0.3,**1**,3]	[0.01, 0.03, **0.1**, 0.3,1,3]
Reg. param. γ	[0.01, **0.03**, 0.1, 0.3,1,3]	[0.01, **0.03**, 0.1, 0.3,1,3]
Min. child weight	[0.01, 0.03, 0.1, 0.3,1,**3**]	[**0.01**, 0.03, 0.1, 0.3,1,3]
Subsample	[0.6, **0.8**]	[0.6, **0.8**]
Col. sample by tree	[0.6, **0.8**]	[**0.6**, 0.8]

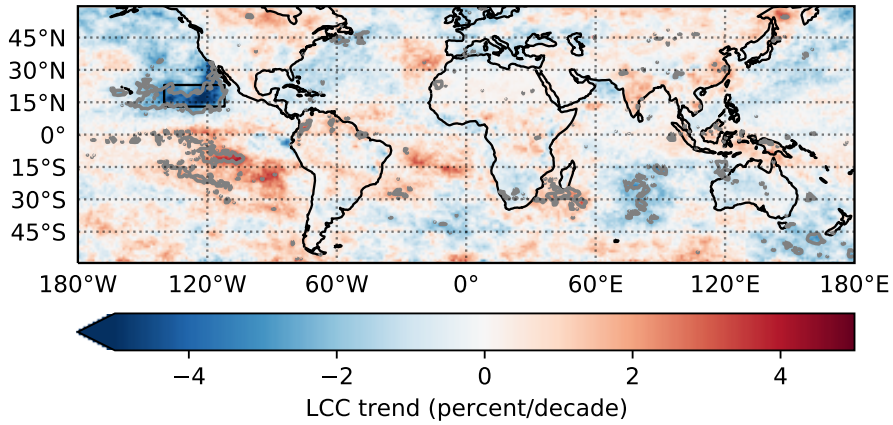

Figure S1. Global LCC trend patterns in the MODIS data between 2001 and 2020. The grey contour marks regions where trends are highly significant (p value < 0.01).

Table S2. Hyperparameter tuning of the ANN model. The left-hand column names the property, and the right-hand column lists the values tested using random grid search for 100 iterations. Bold values are chosen for the final model on the basis of a 10-fold cross validation.

Hyperparameter	**ANN with 6 CCFs**	**ANN with 7 CCFs**
Learning rate	[0.001,0.003,**0.01**,0.03,0.1,0.3]	[0.001,**0.003**,0.01,0.03,0.1,0.3]
Architecture (1–4 layers with [3, 10, 30 and/or 100] neurons (64 possible combinations))	**(30, 100, 3)**	**(30, 100, 3, 10)**
Activation function	[tanh, **relu**]	[tanh, **relu**]
Solver	[sgd, **adam**]	[sgd, **adam**]

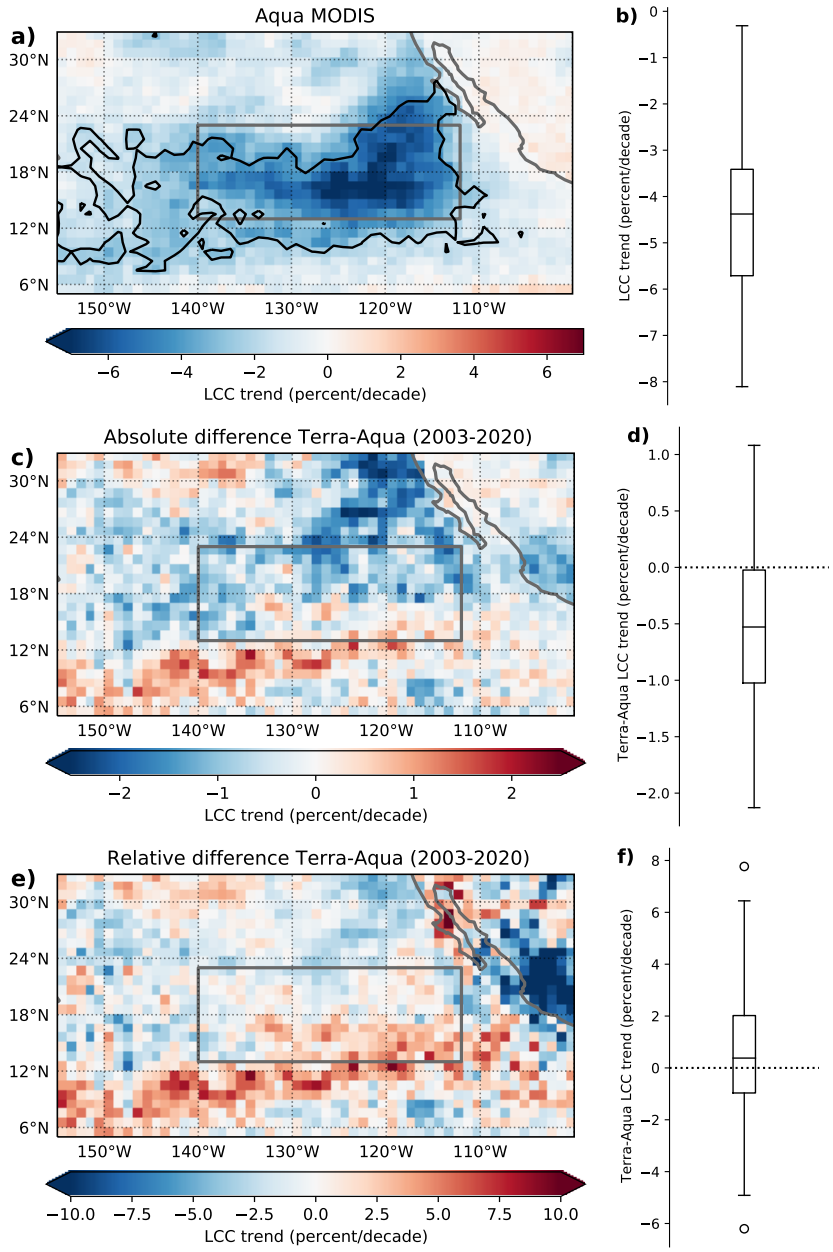

Figure S2. a) Trend patterns of LCC between 2003 and 2020 in the Aqua MODIS data. The black contour marks the regions where the trends in LCC are highly significant (p value < 0.01). The grey box marks the study area, for which the distribution of LCC trends is shown in panel b). Panels c) and d) show the absolute difference between Terra and Aqua MODIS LCC trends for the years with common observations (2003–2020), and panels e) and f) show the same for relative differences.

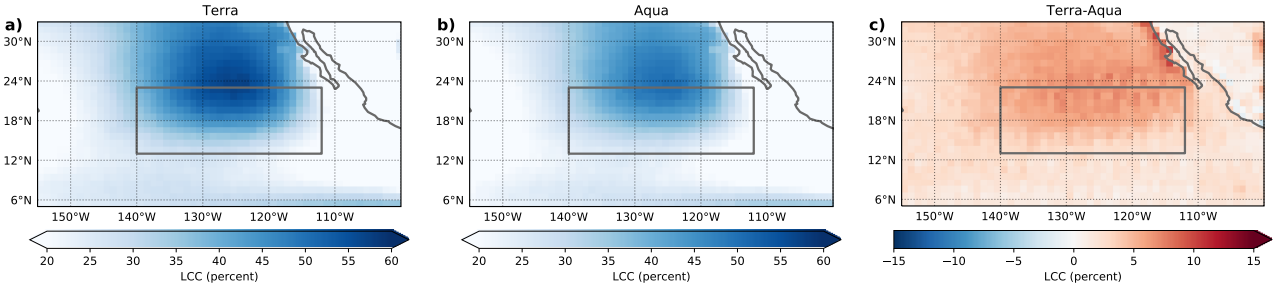

Figure S3. Average LCC of Terra (a)), Aqua (b)), and their difference (c)) for the time period with mutual data (2003–2020).

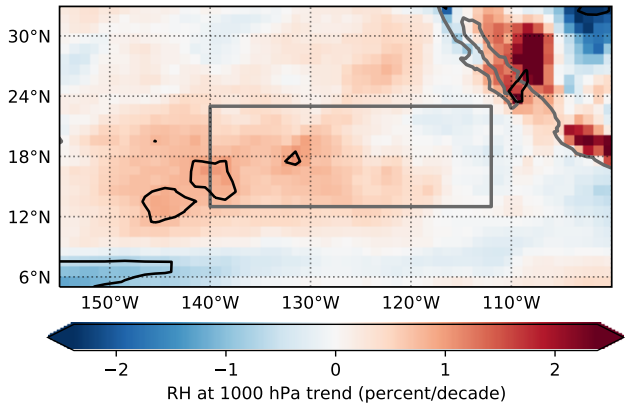

Figure S4. Trend patterns of RH at 1000 hPa in ERA5 between 2001 and 2020. The black contour marks regions where trends are highly significant (p value < 0.01). The figure shows that the significant increase in Q_{diff} cannot be explained by trends in MBL RH.

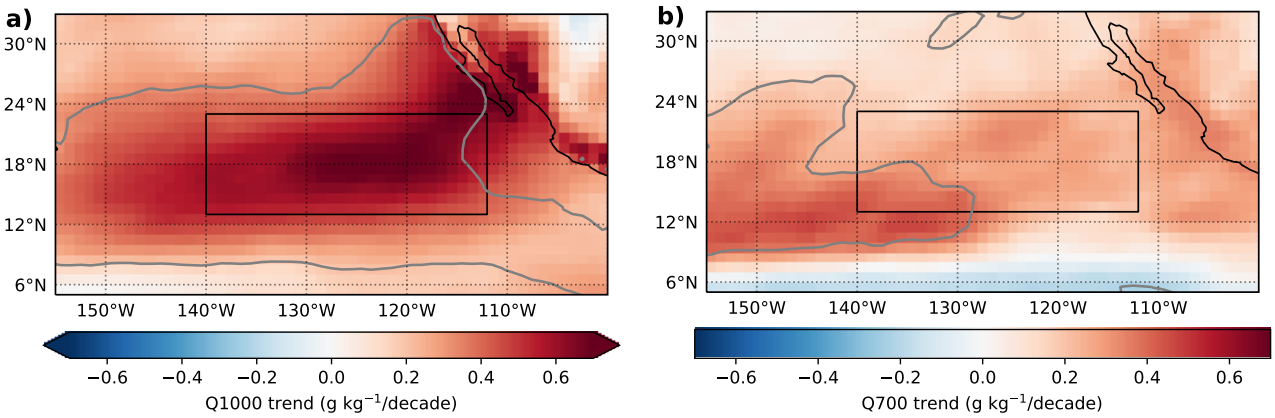

Figure S5. Trend patterns of Q1000 and Q700 in ERA5 between 2001 and 2020. The grey contour marks regions where trends are highly significant (p value < 0.01). The figure shows that the significant increase in Q_{diff} in the NE Pacific is driven by an increase in boundary layer moisture.

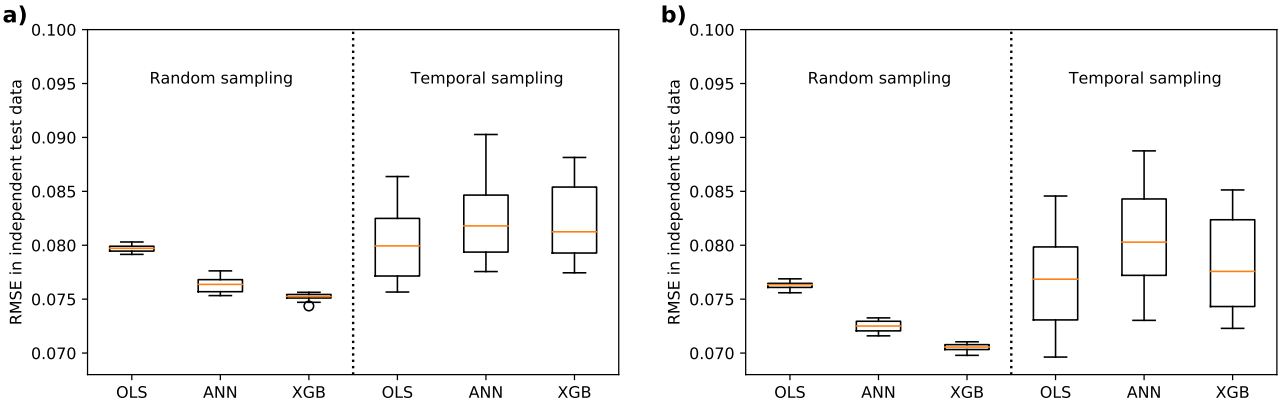

Figure S6. Root mean square error in the independent test data between the random and temporal sampling techniques, and for the 6-CCF (a) and 7-CCF (b) setups.